Journal Pre-proof

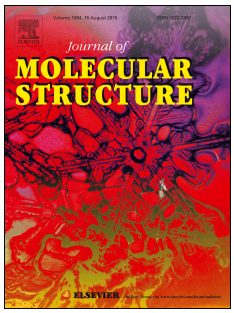

Experimental and theoretical approach to the corrosion inhibition of mild steel in acid medium by a newly synthesized pyrazole carbothioamide heterocycle

F. Boudjellal, H.B. Ouici, A. Guendouzi, O. Benali, A. Sehmi

PII: S0022-2860(19)31151-2

DOI: https://doi.org/10.1016/j.molstruc.2019.127051

Reference: MOLSTR 127051

To appear in: *Journal of Molecular Structure*

Received Date: 16 May 2019

Revised Date: 15 August 2019

Accepted Date: 8 September 2019

Please cite this article as: F. Boudjellal, H.B. Ouici, A. Guendouzi, O. Benali, A. Sehmi, Experimental and theoretical approach to the corrosion inhibition of mild steel in acid medium by a newly synthesized pyrazole carbothioamide heterocycle, *Journal of Molecular Structure* (2019), doi: https://doi.org/10.1016/j.molstruc.2019.127051.

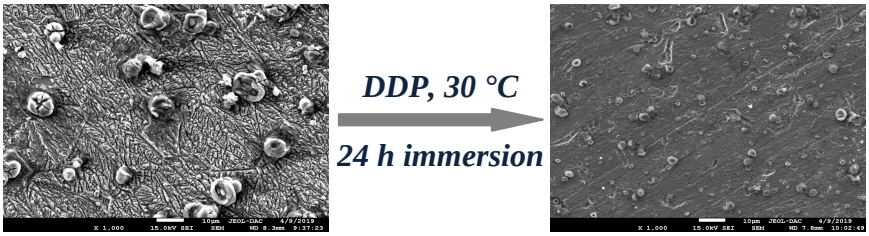

MS + 1 M HCl

MS + 1 M HCl + DDP

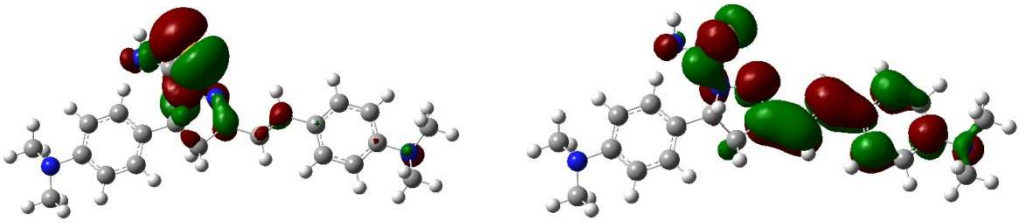

DDP (HOMO)

DDP (LUMO)

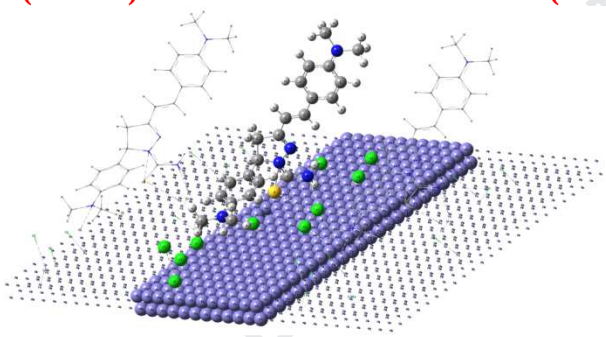

Experimental and theoretical approach to the corrosion inhibition of mild steel in acid medium by a newly synthesized pyrazole carbothioamide heterocycle

F. Boudjellal[1], H. B. Ouici[1], A. Guendouzi[1], O. Benali[2], A. Sehmi[1]
[1]Department of Chemistry, Faculty of Science, University of Saida, Algeria.
[2]Department of Biology, Faculty of Science, University of Saida, Algeria
E-mail : ouici.houari@yahoo.fr

Abstract

Heterocyclic compound such as 3,5-disubstitued pyrazole carbothioamide was synthesized by cyclocondensation reaction between chalcone derivative and thiosemicarbazide as nucleophile substrate in ethanolic sodium hydroxide solution. The structure of synthesized compound namely, (E)-5-(4-(dimethylamino)phenyl)-3-(4-(dimethylamino)styryl)-2,3-dihydro-1H-pyrazole-1-carbothioamide (DDP) was confirmed by infrared FT-IR, ^{1}H NMR and ^{13}C NMR spectra. The inhibitory action was investigated using the gravimetric and electrochemical methods. The results show the strong adsorption of target molecule on the surface of mild steel. The adsorption of (DDP) molecules on the steel surface follows the Langmuir adsorption isotherm and the calculated ($\Delta G°_{ads}$) values of the synthesized inhibitor suggested that the adsorption of this compound involves two types of interaction, chemisorption and physisorption. The polarization curves showed that the (DDP) act as mixed type inhibitor. The SEM analysis reveals that the corrosion inhibition is due to the formation of a protective film on the metal surface. DFT calculations were performed to illustrate the relationship between the molecular structure of (DDP) and their inhibitory properties.

Keywords: Pyrazole, Mild steel, Corrosion, Inhibition, DFT.

1. Introduction:

The hydrochloric acid solutions are widely used in several industrial processes, such as pickling, descaling, acid cleaning, oil well acidizing, etc [1]. Because of their aggressiveness, the use of corrosion inhibitors is considered as the most effective method for the protection of many metals against acid attack and reduces the dissolution of metals [2]. The organic compounds are known to be applicable as corrosion inhibitors for steel in acidic environments. Heterocyclic compounds are organic molecules containing functional groups with heteroatom's, which considerate as efficient inhibitors against metal corrosion in acidic environments [3, 4]. These molecules can easily adsorbed on the metal surface and form a bond between their heteroatom's and the metal surface, thereby reducing the corrosion rate in acidic solutions [5–7]. Pyrazole derivatives are better known, and more widely studied by researchers because of their many important chemical and biological properties [8], they have been commonly used in medicinal chemistry [9-13]. In addition to these biological activities, this family of organic compounds has nitrogen and sulfur heteroatom in their molecular structure as well as pyrazole ring with benzene moieties which can create the inhibition properties in acidic medium and can be strongly adsorbed onto the surface [14, 15]. In our previous study, we have exploited the inhibitory properties of two compounds of pyrazole carbothioamide (DPC and DPCM), which show a high protective action for mild steel in 1 M HCl solution [14]. Moreover, only a few studies using pyrazole carbothioamide derivatives as corrosion inhibitor can be found. These compounds are considered as green corrosion inhibitors because they have lower toxicity with high solubility in acidic environments compared to other organic compound families. Also, this type of organic compounds can easily obtain with a good yield and high purity from chalcone derivatives [14, 16]. The pyrazole entity is often found in many biologically active molecules [17, 18].

The aims of the present work is to synthesis and examine the inhibitory properties of new pyrazole heterocyclic compound containing carbothioamide entity as substituent in their structure for the corrosion inhibition of mild steel in 1 M HCl solution. Effect of concentration, temperature and immersion time on the inhibitory efficiency of pyrazole has been studied systematically. Thermodynamic and kinetic parameters were calculated to predict the inhibition mechanism. Furthermore, the adsorption of inhibitor on the steel surface was discussed by using the electrochemical measurements. The surface morphology of steel samples without and with (DDP) in the electrolytic solution was observed to confirm the presence of the film or the layer formed by the adsorption of (DDP) molecules on mild steel surface using scanning electron microscopy (SEM). Finally, the effect of the structural parameters on inhibitory efficiency has also been studied using (DFT) calculations.

The structure of target pyrazole namely, (E)-5-(4-(dimethylamino)phenyl)-3-(4-(dimethylamino)styryl)-2,3-dihydro-1H-pyrazole-1-carbothioamide (DDP) is given in the Fig. 1.

2. Materials and methods

2. 1. Reagents and spectral analysis

All chemicals used in this study were supplied by Sigma-Aldrich and Merck. Melting points were determined using a Böetius apparatus and are uncorrected. The infrared spectra were registered with a Vertex 70 Bruker spectrometer using potassium bromide disc technique and the results are expressed in wave number (cm^{-1}). The nuclear magnetic resonance (^{1}H NMR and ^{13}C NMR) spectra were registered on a Varian Gemini 300 BB spectrometer working at 300 MHz for ^{1}H NMR and 75 MHz for ^{13}C NMR, using DMSO-*d*6 as the

solvent. Chemical shifts are expressed in δ (ppm) using TMS as the internal standard. The heterocyclic compound was synthesized in accordance with the method described in the literature [19].

2. 2. Mild steel material

Tests were performed on a freshly prepared sheet of DC06EK mild steel of composition *(wt %)* given in the Table 1. Specimens used in all the experiments were mechanically cut into 20 mm × 15 mm × 2 mm dimensions, and then abraded with SiC abrasive papers 200, 400, 600, 800 and 1000 grit respectively, washed in absolute acetone, dried in room temperature and stored in moisture free desiccators.

2. 3. Inhibitor and solution

Fig. 1 shows molecular structure of the heterocyclic compound used in this study named as, (E)-5-(4-(dimethylamino)phenyl)-3-(4-(dimethylamino)styryl)-2,3-dihydro-1H-pyrazole-1-carbothioamide (DDP). The titled compound was synthesized from the reactions described in scheme 1 and 2. The electrolyte solution, 1 M HCl was prepared by dilution of analytical grade 37% HCl with bi-distilled water. The solution was used for all experimental purposes. The concentration range of target inhibitor used in this study was 10^{-5} M, 5×10^{-5} M, 10^{-4} M and 5×10^{-4} M, respectively.

2. 4. Weight loss and electrochemical measurements

Weight loss measurements were carried out in solution of 1 M HCl acid in the absence and the presence of (DDP) inhibitor on mild steel. Sheets with dimensions 20 mm × 15 mm × 2 mm were used. They were polished successively with different grades of emery paper up 1200 grade. Each run was carried out in a glass vessel containing 100 ml of the test solution. A clean weight mild steel sample was completely immersed at an inclined position in the vessel. After 1 h of immersion in 1 M HCl without and with addition of inhibitor at different temperatures (30, 40, 50 and 60°C), the specimen was withdrawn, rinsed with distilled water, washed with acetone, dried and weighed. The weight loss was used to calculate the corrosion rate *(v)* in mg/cm^2.h from the following equation [20]:

$$v = \frac{\Delta w}{S.t} \tag{1}$$

Where *Δw* is the average weight loss of three mild steel sheets, *S* the total area of one steel specimen, and *t* is the immersion time 1 h. With the calculated corrosion rate, the inhibition efficiency *(%IE)* was calculated as follows:

$$\%IE = \frac{v_0 - v}{v_0} \times 100 \tag{2}$$

Where v_0 and v are the corrosion rate of the mild steel coupons in the absence and presence of (DDP), respectively.

Electrochemical experiments were carried out in a glass cell consisting of a platinum electrode (CE) and a saturated calomel electrode (SCE) was used as a counter electrode and a reference electrode, respectively. The mild steel as working electrode with reactive surface area 1 cm^2 was used for electrochemical studies. The potentiodynamic current–potential curves were recorded by changing the electrode potential automatically from -750 mV to -350 mV with a scanning rate of 0.5 mV.s^{-1}. The ac impedance measurements were performed at corrosion potentials *(E_{corr})* over a frequency range of 10 kHz–40 mHz, with a signal amplitude perturbation of 10 mV. Nyquist plots were obtained.

2. 5. SEM surface morphology analysis

A JEOL (JSM-7001F) SEM was used to observe the surface morphology of the mild steel specimens with and without (DDP) in 1 M HCl solution after 24 h of immersion. Mild steel samples used for SEM surface analysis were cut into 20 mm × 15 mm × 2 mm dimensions. They were abraded with SiC abrasive papers 200, 400, 600, 800 and 1000 grit respectively, the specimens were immersed for 24 h in the solution of 1 M HCl without and with optimum concentration 5×10^{-4} M of (DDP) inhibitor at 30 °C, and washed with acetone and distilled water, dried in warm air.

2. 6. DFT quantum calculations

To investigate the correlation between the molecular structure of (DDP) and its inhibition properties, a quantum chemical study has been performed. Geometric structures and electronic properties of (DDP) pyrazole have been calculated by GAUSSIAN 09W software [21], using the Becke's three-parameter hybrid density functional B3LYP method with the standard 6-31G* basis set [22].

The interaction and binding energy *(E_{Int}, E_{Bind})* between the target inhibitor and the Fe (1 1 0) surface was calculated for the minimum energy configuration with the basis set superposition error (BSSE) and evaluated using the counterpoise method to eliminate basis functions overlap effects using equation (3) and (4) [21, 23]:

$$E_{Int} = E_{Inh\,-\,Fe} - (E_{Inh} + E_{Fe}) \quad (3)$$

$$E_{Bind} = -E_{Inh} \quad (4)$$

Where E_{Inh-Fe} is the total energy of the iron crystal together with the adsorbed inhibitor molecule, E_{Inh} and E_{Fe} are the total energy of the free inhibitor molecular and the iron crystal, respectively.

3. Results and discussions

3. 1. Synthesis of pyrazole carbothioamide (DDP)

The target pyrazole (DDP) was synthesized in two steps. The synthetic pathway followed for the preparation of the title compound was accomplished as shown in Scheme 1 and 2. The key intermediate such as dibenzalacetone (4-DBA) employed in the synthesis of the target pyrazole (DDP) was prepared according to a literature method [24]. Thus, dibenzalacetone (4-DBA) was synthesized by the *Claisen-Schimidt* reaction between propanone (acetone) and 4-N,N-dimethylaminobenzaldehyde using ethanol as solvent in the presence of sodium hydroxide as a catalysts. This compound was converted to the corresponding pyrazole carbothioamide (DDP) by refluxing with thiosemicarbazide hydrochloride in ethanol as solvent. Whereas, the cyclocondensation of thiosemicarbazide with dibenzalacetone (4-DBA) at reflux conditions yielded (DDP) after has been neutralized with water ice to give the pyrazole in good yield. Finally, the synthesized compound was recristallized from an ethanol/water (4:1) mixture. The purity of the synthesized compounds (4-DBA) and (DDP) was confirmed by using thin layer chromatography. Moreover, the melting point technique was used to determine the melting points of these compounds. The comparison of the spectroscopic data of the new compounds (Scheme 1 and 2) with those of the previously reported analogues further confirmed the above structure. The pyrazole (DDP) prepared was tested in the following of this work as a corrosion inhibitor of mild steel in 1 M HCl medium.

3. 1. 1. Synthesis of dibenzalacetone derivative (4-DBA) using Claisen-Schimidt condensation

(1.5 g, 0.037 mol) of sodium hydroxide (NaOH) was added to 20 ml of water (H_2O) and 50 ml of ethanol (EtOH) mixture. (12.38 g, 0.033 mol) ml of 4-N,N-dimethylaminobenzaldehyde and 2.5 ml of propanone were added. After 30 min of occasional stirring at room temperature, the product was filtered and the yellow (4-DBA) was recristallized from ethylacetate (yield (75%), mp=192 °C). *^{1}H NMR (DMSO, 300 MHz, δ (ppm)):* 3.04 (s, 12H, $2N(CH_3)_2$), 6.51-7.70 (m, H_a, H_b and 12H, Ar-H). *^{13}C NMR (DMSO, 300 MHz, δ (ppm)):* 190.32 (C_1), 122.46 (C_2), 144.62 (C_3), 124.96 (C_4), 130.53-132.0 (C_5 and C_9), 111.51-112.25 (C_6 and C_8), 40.24 (C_{10}).

3. 1. 2. Synthesis of (E)-5-(4-(dimethylamino)phenyl)-3-(4-(dimethylamino)styryl)-2,3-dihydro-1H-pyrazole-1-carbothioamide (DDP)

A mixture of dibenzalacetone (4-DBA) (3.20 g, 0.01 mol), thiosemicarbazide hydrochloride (1.30 g, 0.01 mol) and sodium hydroxide (NaOH) (0.50 g, 0.0125 mol) was refluxed in 50 ml of ethanol for 6-8 hours. The resultant mixture was concentrated, cooled and poured into crushed ice. The orange solid mass thus separated out was dried and recrystallized from ethanol (yield (77%), mp=185 °C) [25-27]. *^{1}H NMR (DMSO, 300 MHz, δ (ppm)):* 3.36 (s, 12H, $2N(CH_3)_2$), 6.51-7.04 (dd, 1H, C_2–H_a of pyrazole), 6.51-7.04 (dd, 1H, C_2–H_a of pyrazole), 6.51-7.04 (dd, 1H, C_3–H_b of pyrazole), 7.48-8.00 (m, 8H of Ar-H), 11.18 (s, 2H, NH_2). *^{13}C NMR (DMSO, 300 MHz, δ (ppm)):* 152 (C_1), 63.22 (C_3), 177.44 (C_4), 121-130 (C_5, C_6), 40.22 (C_7).

The structure of compound (DDP) was confirmed by their FT-IR, ^{1}H NMR and ^{13}C NMR spectra. The FT-IR absorptions due to the thione group (C=S) in (DDP) appeared at 1071.82 cm^{-1} (str) and 658.8 cm^{-1} [27]. The amine ($-NH_2$) group in (DDP) appeared at 3479.08-3344.21 cm^{-1}, respectively. The absorption bands associated with other functional groups present all appeared in the expected regions. The ^{1}H NMR spectra of substitued pyrazole in DMSO-d^6 exhibited a multiplet in the aromatic region at 7.48-8.00 ppm corresponding to the aromatic hydrogen's protons (Ar-H). The formation of the pyrazole ring is confirmed by the presence of the imine (C=N) function at 1574.9 cm^{-1} in FT-IR spectrum of (DDP). Furthermore, the proton (H_a) and proton (H_b) of pyrazole ring will appear in the region of 6.51-7.04 ppm as a multiplet in ^{1}H NMR spectrum of (DDP). The signals obtained from ^{1}H NMR spectra further confirmed the proposed structure of pyrazole; the primary amine function ($-NH_2$) of carbothioamide entity ($-CSNH_2$) resonate at 11.18 ppm. It should be noted that the ^{1}H NMR and ^{13}C NMR spectrums of pyrazole showed a characteristic signal at 3.36 ppm and 40.22 ppm respectively, matched the six protons of methyl group of the substituent dimethylamino ($-N(CH_3)_2$). Finally, the presence of thione group (C_4=S) is confirmed by the presence of a signal at 177.44 ppm in the ^{13}C NMR spectrum according to the literature [28].

3. 2. Effect of DDP concentration on mild steel corrosion in 1 M HCl

Studying of the corrosion behavior of mild steel in 1 M HCl at 30 °C is represented in Fig. 2. As shown from this figure, by increasing the concentration of this derivative, the corrosion rate *(v_{corr})* of mild steel in 1 M HCl was decreased. This means that the presence of (DDP) retards the corrosion of mild steel in 1 M HCl or in other words, this heterocyclic derivative act as inhibitor.

The values of inhibition efficiency of investigated inhibitor are given in Table 2. From this table and Fig. 2, we can observe, that the inhibition efficiency increases *(%IE)* with increasing the concentration of pyrazole. The maximum *(%IE)* of 96.60% was achieved at (5×10^{-4} M) at 30 °C. The results indicate that (DDP)

is more efficient in the 1 M HCl solution. The high inhibitive performance of this type of heterocyclic compound suggests a higher bonding of pyrazole ring to the surface, which posse's higher number of lone pairs from heteroatom's (S and N) and (π) orbitals [29-31].

3. 3. Effect of temperature on inhibition efficiency of (DDP)

The influence of temperature on inhibition efficiency evolution was studied by weight loss measurements at 30, 40, 50, and 60 °C containing different concentrations of (DDP) pyrazole (Table 3). Fig. 3 shows the variation of inhibition efficiency with temperature. This indicates that inhibition efficiency *(%IE)* increases with inhibitor concentration but decreases with temperature. Which can be attributed to that the higher temperatures might cause desorption of inhibitor molecules from the steel surface [32].

The values of inhibition efficiency obtained from the weight loss for different temperatures in 1 M HCl are given in Table 3. The results show that the maximum *(%IE)* was about (96.60%, 5×10^{-4} M) and (96.30%, 5×10^{-4} M) at 30 °C and 60 °C, respectively, which indicated that (DDP) was a good inhibitor in 1 M HCl at this concentration 5×10^{-4} M [33, 34]. Also, a decrease in inhibition efficiency values with rise in temperature may be due to the physically adsorption (low energy bonds) of inhibitor molecules on the metal surface under study [35].

The relationship between the corrosion rate (v_{corr}) of mild steel in acidic media and absolute temperature *(T)* is often expressed by the Arrhenius equation [35]:

$$\ln v = \ln A - \frac{E_a}{RT} \tag{5}$$

Where v_{corr} is the corrosion rate, E_a is the apparent activation energy, R is the molar gas constant (8.314 J/K.mol), T is the absolute temperature, and A is the frequency factor. The plots of $ln(v_{corr})$ against $(1/T)$ for mild steel corrosion in 1 M HCl in the absence and presence of different concentrations of (DDP) are given in Fig. 4. Apparent activation energy values in the absence and presence of (DDP) at different temperatures were calculated from $ln(v_{corr})$ *vs.* $(1/T)$ plots are given in Table 4.

The data in Table 4 show that all the linear regression coefficients (R^2) are very near to 1, which illustrate that the linear relationship between $ln(v_{corr})$ and the inverse of the absolute temperature $(1/T)$ is good. Also, the value of (E_a) in the presence of (DDP) is higher than that in the uninhibited 1 M HCl solution. It can be observed that the activation energy parameters for corrosion process increases from 54.84 kJ/mol to 80.41 kJ/mol in the absence and the presence of (DDP), respectively. This result shows that the addition of inhibitor significantly reduced the dissolution of metal in the hydrochloric acid media [36]. According to the literature the higher (E_a) in presence of inhibitor for mild steel in comparison with blank solution is due to the electrostatic interactions (physisorption process) of molecules at electrode surface. In addition, the low value of the activation energy (60.21 kJ/mol) at the optimum concentration (5×10^{-4} M) results in the stability of the formed complex (Metal-DDP) at the interface metal/solution [37, 38].

3. 4. Effect of immersion time on surface activity of (DDP)

Effect of immersion time for 30 to 1440 minute on inhibition efficiency of (DDP, 5×10^{-4} M) on the corrosion of mild steel in 1M HCl at 30 °C was studied using weight loss measurements. Table 5 shows the variation of corrosion rates and inhibition efficiency *(%IE)* with time in the absence and presence of (DDP) inhibitor. The Table 5 illustrates that the corrosion rate of mild steel is greatly decreased with immersion time in the presence of (DDP) inhibitor, the corrosion rate *(v_{corr})* value was about (0.03046 mg/cm^2.h at 30 min) and decreased towards (0.00840 mg/cm^2.h and 0.00980 mg/cm^2.h) at (480 min and 1440 min), respectively. This phenomenon may be associated to the progressive adsorption of (DDP) molecules on the steel surface, while in the absence of (DDP) inhibitor the corrosion rate of mild steel was slightly decreased with immersion time from (0.56 mg/cm^2.h at 30 min) to (0.42 mg/cm^2.h and 0.52 mg/cm^2.h) at (480 min and 1440 min), respectively. This behavior may be due to the formation of a passive film of corrosion product $Fe(OH)_2$ on the steel surface, which decreases the corrosion rate of the steel. However, this film formed by $Fe(OH)_2$ molecules can easily be dissolved in the hydrochloric acid solution [36]. Also, results in Table 5 show that the effect of immersion time on inhibition efficiency of (DDP) at 30 °C. In the presence of inhibitor, increasing time resulted in increasing *(%IE)* in 30–1440 min and attains a maximal value 98% after 1440 min. In general, the inhibition efficiency is slightly changed with time immersion time. This reveals that the adsorptive organic layer of (DDP) becomes very compact and uniform at longer immersion time [39, 40].

3. 5. Thermodynamic parameters

It should be noted that the protection of metals against corrosion by using of organic compounds is explained by their adsorption on the metal surface. The latter is well known in three forms: physical adsorption, chemisorptions or mixed adsorption (physisorption with chemisorptions) [41]. The adsorption phenomenon can be implemented by studying the adsorption isotherms.

In order to study the variation of the adsorbed amount with the inhibitor concentration, assuming the increase of the inhibition is attributable to the adsorption of (DDP) on the mild steel surface and obeys Langmuir adsorption isotherm mode, according to the following equation [42]:

$$\frac{C_i}{\theta} = \frac{1}{K_{ads}} + C_i \qquad (6)$$

Where C_i is the concentration of inhibitor, K_{ads} the adsorptive equilibrium constant and θ is the surface coverage calculated as follows [43]:

$$\theta = \frac{v_0 - v}{v_0} \qquad (7)$$

Where v_0 and v the corrosion rate in the absence and presence of (DDP), respectively.

The linear regressions parameters between (C_i/θ) and (C_i) are given in Table 6. Straight lines of (C_i/θ) vs (C_i) at different temperatures 30, 40, 50 and 60 °C are illustrated in Fig. 5 and Fig. 6. It is clear that all linear correlation coefficients (R^2) and slopes values are equal to (1), which indicates that the adsorption of (DDP) on mild steel surface is perfectly follows Langmuir adsorption isotherm at all used temperatures [44-47]. The adsorptive equilibrium constant (K_{ads}) values are calculated from the reciprocal of the intercept of (C_i/θ) as (C_i). It is related to the standard free energy of adsorption (ΔG°_{ads}) as shown the following equation [48]:

$$K_{ads} = \frac{1}{55.5}\exp\left(-\frac{\Delta G^{0}_{ads}}{RT}\right) \quad (8)$$

Where R is the gas constant (8.314 J/K.mol), T the absolute temperature K_{ads}, the value *55.5* is the molar concentration of water in solution [44]. The values of K_{ads} and $\Delta G°_{ads}$ of (DDP) at 30, 40, 50 and 60 °C are listed in Table 6.

The negative values of $(\Delta G°_{ads})$ confirmed that the adsorption of (DDP) molecule on steel surface is a spontaneous process. Generally, values of $(\Delta G°_{ads})$ up to -20 kJ/mol are consistent with the electrostatic interaction between the charged molecules and the charged metal (physical adsorption) while those more negative than -40 kJ/mol involve sharing or transfer of electrons from the inhibitor molecules to the metal surface to form a coordinate type of bond (chemisorption) [49-52]. In the present work, the parameters of $(\Delta G°_{ads})$ are around –43.00, -43.55, -44.65 and -43.74 kJ/mol for (DDP) at 30, 40, 50 and 60 °C, respectively. The results suggested that the adsorption of heterocyclic pyrazole on surface involves the chemical adsorption process. Indeed, the corrosion inhibition of mild steel in 1 M HCl in the presence of target pyrazole is mainly attributed to physical adsorption; this finding is justified by the slight decrease in inhibition efficiency *(%IE)* with increasing temperature. Table 6, also shows that (K_{ads}) of (DDP) is higher than that of other molecules (DPC and DPCM) of the same family, which confirmed that (DDP) is strongly adsorbed on steel surface under study [53, 54]. The presence of heteroatom's, conjugate system with (π) band, pyrazole ring as well as the aromatic substituants in (DDP) structure promotes the sharing of electron (charge transfer) between inhibitor molecules and the vacant iron (d) orbital to establish coordinate type bonds (chemisorption). The electrostatic interactions (physisoprtion) can take place between the charged (DDP) molecules **(DDP-H)**$^{+}$ and the chloride ions **(Cl^{-})** adsorbed at the interface of the electrode interface. From these results, the adsorption process of (DDP) on the surface can be presented as follows (Fig. 7).

3. 6. Potenciodynamic polarization curves

Fig. 8 shows the potentiodynamic polarization curves for MS in 1 M HCl at different concentrations of (DDP) at 30 °C. The addition of (DDP) inhibitor to the 1 M HCl solution leads to a decrease in the corrosion rate and change dramatically the anodic and cathodic curves to lower values of current densities. This indicates that the both cathodic and anodic reactions of MS electrode corrosion were affected by the presence of (DDP) in HCl solution.

Electrochemical parameters of the kinetics corrosion process were calculated from extrapolation of the linear Tafel lines to the corrosion potential and the results are given in Table 7. The inhibition efficiency *(%IE)* was defined as:

$$\%IE = \frac{I_0 - I}{I_0} \times 100 \quad (9)$$

Where I_0 and I represent corrosion current density values without and with (DDP) inhibitor, respectively, determined by extrapolation of Tafel lines to the corrosion potential.

Table 7 shows that an increase in (DDP) concentration is resulted in increased inhibition efficiency to reach a maximum value of 95.50% at 5×10^{-4} M. The results in Table 7 reveal that, increasing of (DDP) concentration leads to the change in potential *(E_{corr})* values toward more positive potential and the values of corrosion current density decreased indicating the surface activity of this type of pyrazole. In addition, we can see that the shift in corrosion potential is around (52.3, 58.9, 89.3, and 115.2 mV) for (10^{-5}, 5 x 10^{-5}, 10^{-4} and 5 x 10^{-4} M), respectively. Indeed, some authors reported that the shift in *(E_{corr})* is higher than 85 mV compared to the blank solution, indicating that the inhibitor is regarded as a cathodic or anodic type inhibitor, while the displacement is lower than 85 mV, the inhibitor is considered as a mixed type. In this study we can observe that the values of shift in *(E_{corr})* at (10^{-4} and 5 x 10^{-4} M) are higher than 85 mV, but at the concentration of (10^{-5} and 5 x 10^{-5} M) the values of shift in *(E_{corr})* are lower than 85 mV, which mean that the (DDP) can considered as a mixed type inhibitor with predominant anodic effectiveness [55]. The values of both anodic and cathodic Tafel slopes are slightly changed with the (DDP) inhibitor addition, indicating that the inhibitors retarded the mild steel dissolution by simple blocking the anodic and cathodic sites of the corrosion reaction on the steel surface, without changing the mechanism of corrosion process [56].

The corrosion of mild steel in HCl solution can be presented as follows [57, 58]: The anodic dissolution reaction of iron in the presence of chloride anion in hydrochloric acid solution.

$$Fe + Cl^- \longrightarrow (FeCl^-)_{ads} \quad (10)$$

$$(FeCl^-)_{ads} \longrightarrow (FeCl)_{ads} + e^- \quad (11)$$

$$(FeCl)_{ads} \longrightarrow (FeCl^+) + e^- \quad (12)$$

$$FeCl^+ \longrightarrow Fe^{2+} + Cl^- \quad (13)$$

On the other hand, the cathodes H_2 evolution can be represented as:

$$Fe + H^+ \longrightarrow (FeH^+)_{ads} \quad (14)$$

$$(FeH^+)_{ads} + e^- \longrightarrow (FeH)_{ads} \quad (15)$$

$$(FeH)_{ads} + H^+ + e^- \longrightarrow Fe + H_2 \quad (16)$$

It is generally accepted that the mechanism of adsorption process involves the replacement of water molecules adsorbed at the surface of the metal.

$$Inh_{(sol)} + nH_2O \longleftrightarrow Inh_{(ads)} + nH_2O_{(sol)} \quad (17)$$

Where *(n)* is the size ratio, that is, the number of water molecules replaced by one organic inhibitor. The inhibitor molecules may then combine with freshly generated Fe^{2+} to forming metal–inhibitor complexes, according to Equation (18). Therefore, it is possible to suggest that the presence of chloride ion (Cl^-) on the steel surface can facilitate the adsorption of the positive complex through to the electrostatic interactions [59].

$$Fe^{2+} + Inh_{(ads)} \longrightarrow [Fe\text{-}Inh]^{2+}_{ads} \quad (18)$$

3. 7. Electrochemical impedance spectroscopy (EIS)

The Nyquist and Bode Modulus plots for MS in 1 M HCl at 30 °C in the absence and presence of various concentrations of pyrazole inhibitor are given in Fig. 9 and Fig. 10, respectively. These diagrams were obtained after 1 h of immersion in 1 M HCl at 30 °C.

The impedance spectra in the Fig. 9 are presented as semicircle with diameter increases with the increase of (DDP) concentration. This indicates that the corrosion process of mild steel in 1 M HCl is controlled by the charge transfer phenomenon and the addition of (DDP) to electrolytic solution does not change the mechanism of MS corrosion in the acid solution [60]. Also, the obtained impedance plots are not perfect semicircles which are due to the frequency dispersion as a result of the heterogeneity of MS surface. Furthermore, it is clear, from Fig. 9 that the adsorptions of (DDP) on the electrode surface increase the impedance response of MS in comparison with the uninhibited HCl solution [61]. The Fig. 10 illustrates the Bode modulus plot, we can see an increase of the impedance values at low frequencies and that the shape of the curve remains the same without and with the addition of (DDP) to the corrosive solution. This result confirms the evolution of the protective film adsorbed on the steel surface with the increase in the concentration of (DDP) inhibitor [62]. Electrochemical impedances spectra of MS in 1 M HCl are simulated by the equivalent circuit diagram presented in the Fig. 11.

. The electrochemical impedances parameters of charge transfer resistance *(R_{ct})*, double layer capacitance *(C_{dl})* and inhibition efficiency *(%IE)* are given in Table 8. The *(%IE)* is calculated by charge transfer resistance obtained from Nyquist plots, according to the equation (19) [63].

$$\%IE = \frac{R_{ct(inh)} - R_{ct}}{R_{ct(inh)}} \times 100 \qquad (19)$$

Where R_{ct} and $R_{ct(inh)}$ are the charge transfer resistance values without and with (DDP), respectively.

Table. 8 shows that, charge transfer resistance *(R_{ct})* increases with the increasing of (DDP) concentration in the HCl environment. On the other hand, the decreasing values of *(C_{dl})* with the addition of (DDP) compared to that in absence of the inhibitor may be attributed to a lower local dielectric constant, which due the gradual replacement of water molecules by the adsorption of the (DDP) molecules at electrode interface and the formation of organic layer increasing the thickness of the electrical double layer and reduces the surface of mild steel exposed to acidic solution according to Helmholtz equation (20) [64].

$$C_{dl} = \frac{\varepsilon^{\circ}\varepsilon S}{d} \qquad (20)$$

Where S electrode surface, ε^{o} permittivity of air, ε local dielectric constant and d film thickness

The Inhibition Efficiency *(%IE)* increases with the concentration of (DDP) to reaches 95.30 % (5×10^{-4} M) which confirm the effectiveness of this type of pyrazole derivative containing the carbothioamide ($-CSNH_2$) entity in their structure [17]. Also, the phase shift *(n)* values are given in Table 8. Decrease of *(n)* values by the increase of inhibitor concentration compared to the uninhibited solution can be attributed to the increase of the surface inhomogeneity as a result of the (DDP) molecules adsorption [33].

3. 7. Scanning electron microscopy (SEM)

The surface morphology of mild steel in 1 M HCl with and without (DDP) inhibitor was studied by scanning electron microscopy in order to confirm that the corrosion inhibition of MS is due to the formation of an organic layer of (DDP) molecules. Fig. 12 shows the SEM photos of MS surface in 1 M HCl solution after immersion for 24 h in absence and presence of 5×10^{-4} M of (DDP) compound. It can be observed from Fig. 12 (A) a uniform surface along with the presence of some cracks and small black holes, which may be due

to the defect of steel. The Fig. 12 (B) of the MS surface after immersion in uninhibited 1 M HCl shows an aggressive attack of the corroding medium on the steel surface. On the other hand the presence of (DDP) inhibitor in 1 M HCl solution leads to the formation of an organic layer on the surface of steel as shown in Fig. 12 (C). Consequently, the inhibition action of this type of molecule may be related to the formation of a stable film at the interface MS/HCl, with prevents the aggressive attack of the medium on the surface of the steel under study.

4. Quantum Chemical studies

4. 1. DFT calculation

The corrosion inhibition by means of organic compounds depend a several factors, including the structural parameters, such as stereochemistry of the molecule, the electronic density, frontier molecular orbitals and others witch play a decisive role on the mechanism of corrosion inhibition [65, 66]. In general, the organic molecules, especially the heterocyclic compounds containing a particular function groups, heteroatom's and aromatic systems in their structure have high ability to act as corrosion inhibitors. In order to find a relationship between the inhibition efficiency and structural properties of (DDP), some quantum parameters such as dipole moment (μ), total energy (E_{tot}), highest occupied molecular orbital (E_{HOMO}), lowest unoccupied molecular orbital (E_{LUMO}) energies, (E_{LUMO}–E_{HOMO}) energy gap ($\Delta E = E_{LUMO}–E_{HOMO}$) and molecular volume ($V$) were calculated using B3LYP/6-31G* method. The optimized structure, (HOMO, LUMO) electronic distribution and data quantum's are given in the Fig. 13 and Table 9, respectively.

It is clear from this Fig. 13 that the HOMO and LUMO orbital's of (DDP) gives rise to interactions between the inhibitor and metal surface. This figure shows that the electronic density is concentrated on the heteroatom's of pyrazole ring and on the conjugate system of (DDP), which shows that these sites are the best centers for the donor-acceptor process between the inhibitor and (d) orbital of iron under study [67]. The analysis of data in Table 9 shows that the calculated E_{HOMO}, E_{LUMO} and ΔE energies are -5.08 eV, -1.94 eV and 3.14 eV, respectively. According to the FMO (frontier molecular orbital theory), less negative E_{HOMO} energy and the smaller energy gap ($\Delta E = E_{LUMO}–E_{HOMO}$) implies the tendency of the inhibitor molecules to share one or more electrons to the vacant (d) orbital of the iron atoms [68]. Consequently, these results indicate that (DDP) molecules can easily transfer electrons to the vacant (d) orbitals of the iron surface. In other words, the (DDP) molecules have been strongly adsorbed on the steel surface involving the electron sharing to achieve better corrosion inhibition activity compared to other heterocyclic compounds [14, 33, 60]. Also, increasing values of dipole moment ($\mu = 9.72D$) and molecular volume ($V = 340.57\ cm^3/mol$) may facilitate adsorption by influencing the transport process through the adsorbed layer, and promote the electrostatic interaction between the metal charge and the charged molecules of this compound [69]. These results show the performance of (DDP) compared to (DPC, DPCM) molecules of the same pyrazole family [14].

4. 2. Fukui indice analysis

The fukui indices given in Table 10 have been calculated in order to give further insight into the experimental study and to predict the best adsorption sites for nucleophilic and electrophilic exchanges [70]. The data in Table 10 shows that the highest values of (f_k^+) for nucleophilic attack are on N4, S7 and C19 while the highest value of (f_k^-) is on S7, which indicate that these positions are the preferred site for the adsorption of

(DDP) inhibitor on metal surface through donor-acceptor process (Fig. 14). The results obtained are in good agreement with the optimized structure, HOMO and LUMO electronic distribution cited in the Fig. 13, this allows us to calculate the interaction and binding energy for the best disposition of the (DDP) molecule on the iron surface as shown in flowing figure (Fig. 14). The calculated interaction and binding energy values are listed in Table 11.

The calculated interaction energy values of the (DDP-Fe) system in vacuum and HCl solution are respectively; -21.11 and -27.01 kcal/mol. The higher and negative value of interaction energy is due to the strong adsorption of (DDP) molecule on iron surface [71]. Also, the higher positive value of binding energy for target inhibitor (27.01 kcal/mol) suggests that the protective organic film formed by the adsorption of (DDP) at the interface Metal/HCl is stable and adherent to the acid attack. These results confirmed the complementary between experimental data and theoretical quantum methods, which have proved that this type of molecules family can be a good corrosion inhibitor of steel in HCl medium [72].

5. Conclusion

A novel pyrazole heterocyclic derivative namely, (E)-5-(4-(dimethylamino)phenyl)-3-(4-(dimethylamino)styryl)-2,3-dihydro-1H-pyrazole-1-carbothioamide (DDP) was synthesized by cyclocondensation reaction of the corresponding dibenzalcetone (4-DBA) and thiosemicarbazide in sodium hydroxide solution and ethanol solvent. The structures of this compound was determined by FT-IR, ^{1}H NMR and ^{13}C NMR spectra. The compound was tested as inhibitor for corrosion of mild steel in 1 M HCl medium. From the results of different methods used in this study, we can draw the following conclusions:

1- (DDP) acts as a good inhibitor for the corrosion of MS in 1 M HCl. The *(%IE)* values increase with the inhibitor concentration to attain 96.60% at 5×10^{-4} M. While slightly decrease with the temperature.

2- The adsorption of (DDP) on MS surface obeys Langmuir adsorption isotherm. The adsorption process is a spontaneous and the decrease of (K_{ads}) with temperature accompanied by a decrease in inhibition efficiency.

3- The kinetic (E_a) and thermodynamic $(\Delta G°_{ads})$ parameters indicates that the adsorption of pyrazole on MS surface involves both physical adsorption and chemical adsorption.

4- (DDP) pyrazole acts as a mixed type inhibitor in 1 M HCl, and SEM analysis shows that the inhibition mechanism of target inhibitor is due to the formation of organic layer, which effectively protects steel from HCl attack.

5- Optimized molecular structures obtained by quantum chemical calculations illustrate that the (DDP) may be adsorbed on the steel surface involving donor-acceptor interactions between the π-electrons, N and S heteroatom's (pyrazole ring) and the vacant (d) orbitals of iron atoms. Also, the results show a good correlation of dipole moment of (DDP) and it inhibition activity.

6- Interaction energy and binding energy shows that the (DDP) is strongly adsorbed into the iron surface.

Acknowledgement

The author's thanks ministry of higher education and scientific research of Algeria (MESRS) and the HPC ressources of UCI-UABT of the University Abou bekr Belkaïd of Tlemcen for financial support in this research.

References

[1] J. Cruz, R. Martínez, J. Genesca, E. García-Ochoa, Experimental and theoretical study of 1-(2-ethylamino)-2-methylimidazoline as an inhibitor of carbon steel corrosion in acid media, Journal of Electroanalytical Chemistry, 566 (2004) 111-121.

[2] M.A. Migahed, Electrochemical investigation of the corrosion behaviour of mild steel in 2M HCl solution in presence of 1-dodecyl-4-methoxy pyridinium bromide, Materials Chemistry and Physics, 93 (2005) 48-53.

[3] I.I. Bergmann, Corrosion Inhibitors, Macemillan, New York, 1963.

[4] Y.I. Kuznetsov, Organic Inhibitors of Corrosion of Metals, Springer US, 1996.

[5] K.M. Ismail, Evaluation of cysteine as environmentally friendly corrosion inhibitor for copper in neutral and acidic chloride solutions, Electrochimica Acta, 52 (2007) 7811-7819.

[6] M. Benabdellah, R. Touzani, A. Aouniti, A. Dafali, S. El Kadiri, B. Hammouti, M. Benkaddour, Inhibitive action of some bipyrazolic compounds on the corrosion of steel in 1 M HCl: Part I: Electrochemical study, Materials Chemistry and Physics, 105 (2007) 373-379.

[7] H. Ashassi-Sorkhabi, S. Moradi-Alavian, M.D. Esrafili, A. Kazempour, Hybrid sol-gel coatings based on silanes-amino acids for corrosion protection of AZ91 magnesium alloy: Electrochemical and DFT insights, Progress in Organic Coatings, 131 (2019) 191-202.

[8] F.M. Abdelrazek, P. Metz, N.H. Metwally, S.F. El-Mahrouky, Synthesis and Molluscicidal Activity of New Cinnoline and Pyrano [2, 3-c] pyrazole Derivatives, Archiv der Pharmazie: An International Journal Pharmaceutical and Medicinal Chemistry, 339 (2006) 456-460.

[9] M. Messali, M. Larouj, H. Lgaz, N. Rezki, F.F. Al-Blewi, M.R. Aouad, A. Chaouiki, R. Salghi, I.-M. Chung, A new schiff base derivative as an effective corrosion inhibitor for mild steel in acidic media: Experimental and computer simulations studies, Journal of Molecular Structure, 1168 (2018) 39-48.

[10] A. Singh, K.R. Ansari, Y. Lin, M.A. Quraishi, H. Lgaz, I.-M. Chung, Corrosion inhibition performance of imidazolidine derivatives for J55 pipeline steel in acidic oilfield formation water: Electrochemical, surface and theoretical studies, Journal of the Taiwan Institute of Chemical Engineers, 95 (2019) 341-356.

[11] A. Nazarov, N. Le Bozec, D. Thierry, Scanning Kelvin Probe assessment of steel corrosion protection by marine paints containing Zn-rich primer, Progress in Organic Coatings, 125 (2018) 61-72.

[12] H. Idrissi, S. Ramadan, J. Maghnouj, R. Boulif, Modern concept of acoustic emission (AE) coupled with electrochemical measurements for monitoring the elastomer-coated carbon steel damage in phosphoric acid medium, Progress in Organic Coatings, 63 (2008) 382-388.

[13] E.E. Elemike, H.U. Nwankwo, D.C. Onwudiwe, Experimental and theoretical studies of (Z)-N-(2-chlorobenzylidene) naphthalen-1-amine and (Z)-N-(3-nitrobenzylidene)naphthalen-1-amine, and their corrosion inhibition properties, Journal of Molecular Structure, 1155 (2018) 123-132.

[14] H.B. Ouici, O. Benali, A. Guendouzi, Experimental and quantum chemical studies on the corrosion inhibition effect of synthesized pyrazole derivatives on mild steel in hydrochloric acid, Research on Chemical Intermediates, 42 (2016) 7085-7109.

[15] F. El-Taib Heakal, S.K. Attia, S.A. Rizk, M.A. Abou Essa, A.E. Elkholy, Synthesis, characterization and computational chemical study of novel pyrazole derivatives as anticorrosion and antiscalant agents, Journal of Molecular Structure, 1147 (2017) 714-724.

[16] R. A. Gupta, S. G. Kaskhedikar, Synthesis, antitubercular activity, and QSAR analysis of substituted nitroaryl analogs: chalcone, pyrazole, isoxazole, and pyrimidines, Med Chem Res, 22 (2013) 3863–3880

[17] A.M. Farag, N. A. Kheder, K. M. Dawood, A. M. El Defrawy, A facile access and computational studies of new 4,5-biprazole derivatives, Heterocycles, 94 (2017) 1245-1256;

[18] A. M. Farag, A. S. Mayhoub, S. E. Barakat, A. H. Bayomi, Synthesis of new N-phenylpyrazole derivatives with potent antimicrobial activity, Bioorg. Med. Chem, 16 (2008) 4569-4578.

[19] B. Rezessy, Z. Zubovics, J. Kovács, G. Tóth, Synthesis and structure elucidation of new thiazolotriazepines, Tetrahedron, 55 (1999) 5909-5922.

[20] M. Lebrini, M. Traisnel, M. Lagrenée, B. Mernari, F. Bentiss, Inhibitive properties, adsorption and a theoretical study of 3, 5-bis (n-pyridyl)-4-amino-1, 2, 4-triazoles as corrosion inhibitors for mild steel in perchloric acid, Corrosion science, 50 (2008) 473-479.

[21] Gaussian 09, Revision A.1, M.J. Frisch, G.W. Trucks, H.B. Schlegel, G.E. Scuseria, M.A. Robb, J.R. Cheeseman, G. Scalmani, V. Barone, B. Mennucci, G.A. Petersson, H. Nakatsuji, M. Caricato, X. Li, H.P. Hratchian, A.F. Izmaylov, J. Bloino, G. Zheng, J.L. Sonnenberg, M. Hada, M. Ehara, K. Toyota, R. Fukuda, J. Hasegawa, M. Ishida, T. Nakajima, Y. Honda, O. Kitao, H. Nakai, T. Vreven, J.A. Montgomery, Jr., J.E. Peralta, F. Ogliaro, M. Bearpark, J.J. Heyd, E. Brothers, K.N. Kudin, V.N. Staroverov, R. Kobayashi, J. Normand, K. Raghavachari, A. Rendell, J.C. Burant, S.S. Iyengar, J. Tomasi, M. Cossi, N. Rega, J.M. Millam, M. Klene, J.E. Knox, J.B. Cross, V. Bakken, C. Adamo, J. Jaramillo, R. Gomperts, R.E. Stratmann, O. Yazyev, A.J. Austin, R. Cammi, C. Pomelli, J.W. Ochterski, R.L. Martin, K. Morokuma, V.G. Zakrzewski, G.A. Voth, P. Salvador, J.J. Dannenberg, S. Dapprich, A.D. Daniels, O. Farkas, J.B. Foresman, J.V. Ortiz, J. Cioslowski, D.J. Fox, Gaussian, Inc., Wallingford CT, 2009

[22] A.D. Becke, A new mixing of Hartree–Fock and local density-functional theories, The Journal of chemical physics, 98 (1993) 1372-1377.

[23] S.F. Boys, F.d. Bernardi, The calculation of small molecular interactions by the differences of separate total energies. Some procedures with reduced errors, Molecular Physics, 19 (1970) 553-566.

[24] Y.R. Huang, J.A. Katzenellenbogen, Regioselective synthesis of 1, 3, 5-triaryl-4-alkylpyrazoles: novel ligands for the estrogen receptor, Organic letters, 2 (2000) 2833-2836.

[25] S. Hassan, Synthesis, antibacterial and antifungal activity of some new pyrazoline and pyrazole derivatives, Molecules, 18 (2013) 2683-2711.

[26] S. L. Zhu, Y. Wu, C.-J. Liu, C.-Y. Wei, J.-C. Tao, H.-M. Liu, Synthesis and in vitro cytotoxic activity evaluation of novel heterocycle bridged carbothioamide type isosteviol derivatives as antitumor agents, Bioorganic & Medicinal Chemistry Letters, 23 (2013) 1343-1346.

[27] T. A. Mohamed, A. M. Hassan, U. A. Soliman a,1, W. M. Zoghaib, J. Husband, M. M. Abdelall, Infrared, Raman and NMR spectra, conformational stability, normal coordinate analysis and B3LYP calculations of 5-amino-4-cyano-3-(methylthio)-1H-pyrazole-1-carbothioamide, J. Mol. Struct, 985 (2011) 277–291

[28] K. Kumara, N. Shivalingegowda, L.D. Mahadevaswamy, A.K. Kariyappa, N.K. Lokanath, Crystal structure studies and Hirshfeld surface analysis of 5-(4-methoxyphenyl)-3-(thiophen-2-yl)-4,5-dihydro-1H-pyrazole-1-carbothioamide, Chemical Data Collections, 9-10 (2017) 251-262.

[29] H. B. Ouici, M. Belkhouda, O. Benali, R. Salghi, L. Bammou, A. Zarrouk, B. Hammouti, Adsorption and inhibition effect of 5-phenyl-1, 2, 4-triazole-3-thione on C38 steel corrosion in 1 M HCl, Research on Chemical Intermediates, 41 (2015) 4617-4634.

[30] A. Singh, M. Talha, X. Xu, Z. Sun, Y. Lin, Heterocyclic Corrosion Inhibitors for J55 Steel in a Sweet Corrosive Medium, ACS Omega, 2 (2017) 8177-8186.

[31] R. Solmaz, E. Altunbaş, G. Kardaş, Adsorption and corrosion inhibition effect of 2-((5-mercapto-1, 3, 4-thiadiazol-2-ylimino) methyl) phenol Schiff base on mild steel, Materials Chemistry and Physics, 125 (2011) 796-801.

[32] H. Ouici, M. Tourabi, O. Benali, C. Selles, C. Jama, A. Zarrouk, F. Bentiss, Adsorption and corrosion inhibition properties of 5-amino 1,3,4-thiadiazole-2-thiol on the mild steel in hydrochloric acid medium: Thermodynamic, surface and electrochemical studies, Journal of Electroanalytical Chemistry, 803 (2017) 125-134.

[33] H. B. Ouici, O. Benali, A. Guendouzi, Corrosion inhibition of mild steel in acidic media using newly synthesized heterocyclic organic molecules: Correlation between inhibition efficiency and chemical structure, in, AIP Publishing, 2015, pp. 020086.

[34] R. Solmaz, Investigation of the inhibition effect of 5-((E)-4-phenylbuta-1, 3-dienylideneamino)-1, 3, 4-thiadiazole-2-thiol Schiff base on mild steel corrosion in hydrochloric acid, Corrosion Science, 52 (2010) 3321-3330.

[35] E.E. Oguzie, C. Unaegbu, C.N. Ogukwe, B.N. Okolue, A.I. Onuchukwu, Inhibition of mild steel corrosion in sulphuric acid using indigo dye and synergistic halide additives, Materials Chemistry and Physics, 84 (2004) 363-368.

[36] X. Li, S. Deng, H. Fu, G. Mu, Inhibition effect of 6-benzylaminopurine on the corrosion of cold rolled steel in H2SO4 solution, Corrosion Science, 51 (2009) 620-634.

[37] M.M. Osman, R.A. El-Ghazawy, A.M. Al-Sabagh, Corrosion inhibitor of some surfactants derived from maleic-oleic acid adduct on mild steel in 1 M H2SO4, Materials chemistry and physics, 80 (2003) 55-62.

[38] M. Elachouri, M.S. Hajji, M. Salem, S. Kertit, J. Aride, R. Coudert, E. Essassi, Some nonionic surfactants as inhibitors of the corrosion of iron in acid chloride solutions, Corrosion, 52 (1996) 103-108.

[39] I.B. Obot, E.E. Ebenso, I.A. Akpan, Z.M. Gasem, A.S. Afolabi, Thermodynamic and density functional theory investigation of sulphathiazole as green corrosion inhibitor at mild steel/hydrochloric acid interface, Int J Electrochem Sci, 7 (2012) 1978-1996.

[40] S.L. Granese, B.M. Rosales, C. Oviedo, J.O. Zerbino, The inhibition action of heterocyclic nitrogen organic compounds on Fe and steel in HCl media, Corrosion Science, 33 (1992) 1439-1453.

[41] E. Khamis, The effect of temperature on the acidic dissolution of steel in the presence of inhibitors, Corrosion, 46 (1990) 476-484.

[42] X. Li, S. Deng, H. Fu, T. Li, Adsorption and inhibition effect of 6-benzylaminopurine on cold rolled steel in 1.0 M HCl, Electrochimica Acta, 54 (2009) 4089-4098.

[43] I. Sekine, Y. Hirakawa, Effect of 1-hydroxyethylidene-1, 1-diphosphonic acid on the corrosion of SS 41 steel in 0.3% sodium chloride solution, Corrosion, 42 (1986) 272-277.

[44] W.A. Badawy, K.M. Ismail, A.M. Fathi, Corrosion control of Cu–Ni alloys in neutral chloride solutions by amino acids, Electrochimica Acta, 51 (2006) 4182-4189.

[45] A. Azim, L.A. Shalaby, H. Abbas, Mechanism of the corrosion inhibition of Zn Anode in NaOH by gelatine and some inorganic anions, Corrosion Science, 14 (1974) 21-24.

[46] F. Bentiss, M. Bouanis, B. Mernari, M. Traisnel, M. Lagrenee, Effect of iodide ions on corrosion inhibition of mild steel by 3, 5-bis (4-methylthiophenyl)-4H-1, 2, 4-triazole in sulfuric acid solution, Journal of Applied Electrochemistry, 32 (2002) 671-678.

[47] X. Sheng, Y.-P. Ting, S.O. Pehkonen, Evaluation of an organic corrosion inhibitor on abiotic corrosion and microbiologically influenced corrosion of mild steel, Industrial & Engineering Chemistry Research, 46 (2007) 7117-7125.

[48] E. Cano, J.L. Polo, A. La Iglesia, J.M. Bastidas, A study on the adsorption of benzotriazole on copper in hydrochloric acid using the inflection point of the isotherm, Adsorption, 10 (2004) 219-225.

[49] F. Bentiss, M. Lebrini, M. Lagrenée, Thermodynamic characterization of metal dissolution and inhibitor adsorption processes in mild steel/2, 5-bis (n-thienyl)-1, 3, 4-thiadiazoles/hydrochloric acid system, Corrosion Science, 47 (2005) 2915-2931.

[50] W.H. Li, Q. He, S.-t. Zhang, C.-l. Pei, B.-r. Hou, Some new triazole derivatives as inhibitors for mild steel corrosion in acidic medium, Journal of Applied Electrochemistry, 38 (2008) 289-295.

[51] F. Bensajjay, S. Alehyen, M. El Achouri, S. Kertit, Corrosion inhibition of steel by 1-phenyl 5-mercapto 1, 2, 3, 4-tetrazole in acidic environments (0.5 M H_2SO_4 and 1/3 M H_3PO_4), Anti-Corrosion Methods and Materials, 50 (2003) 402-409.

[52] M. Şahin, S. Bilgic, H. Yılmaz, The inhibition effects of some cyclic nitrogen compounds on the corrosion of the steel in NaCl mediums, Applied Surface Science, 195 (2002) 1-7.

[53] P. Singh, A. Singh, M.A. Quraishi, Thiopyrimidine derivatives as new and effective corrosion inhibitors for mild steel in hydrochloric acid: electrochemical and quantum chemical studies, Journal of the Taiwan Institute of Chemical Engineers, 60 (2016) 588-601.

[54] O. Benali, L. Larabi, M. Traisnel, L. Gengembre, Y. Harek, Electrochemical, theoretical and XPS studies of 2-mercapto-1-methylimidazole adsorption on carbon steel in 1 M $HClO_4$, Applied surface science, 253 (2007) 6130-6139.

[55] X. Li, S. Deng, H. Fu, Three pyrazine derivatives as corrosion inhibitors for steel in 1.0 M H2SO4 solution, Corrosion science, 53 (2011) 3241-3247.

[56] C. Cao, On electrochemical techniques for interface inhibitor research, corrosion science, 38 (1996) 2073-2082.

[57] A. Yurt, A. Balaban, S.U. Kandemir, G. Bereket, B. Erk, Investigation on some Schiff bases as HCl corrosion inhibitors for carbon steel, Mater. Chem. Phys. 85 (2004) 420.

[58] W. Li, Q. He, C. Pei, B. Hou, Experimental and theoretical investigation of the adsorption behaviour of new triazole derivatives as inhibitors for mild steel corrosion in acid media, Electrochim. Acta 52 (2007) 6386.

[59] Q.B. Zhang, Y.X. Hua, Corrosion inhibition of mild steel by alkylimidazolium ionic liquids in hydrochloric acid, Electrochim. Acta 54 (2009) 1881–1887.

[60] H.B. Ouici, O. Benali, Y. Harek, S.S. Al-Deyab, L. Larabi, B. Hammouti, Influence of the 2-Mercapto-1-Methyl Imidazole (MMI) on the Corrosion Inhibition of Mild Steel in 5% HCl, Int. J. Electrochem. Sci, 7 (2012) 2304-2319.

[61] M. Lebrini, M. Lagrenée, H. Vezin, M. Traisnel, F. Bentiss, Experimental and theoretical study for corrosion inhibition of mild steel in normal hydrochloric acid solution by some new macrocyclic polyether compounds, Corrosion Science, 49 (2007) 2254-2269.

[62] A.K. Singh, S.K. Shukla, M. Singh, M.A. Quraishi, Mater. Chem. Phys. 129 (2011) 68–76.

[63] Q. Qu, Z. Hao, L. Li, W. Bai, Y. Liu, Z. Ding, Synthesis and evaluation of Tris-hydroxymethyl-(2-hydroxybenzylidenamino)-methane as a corrosion inhibitor for cold rolled steel in hydrochloric acid, Corrosion Science, 51 (2009) 569-574.

[64] A. E. Elkholy, F. Heakal, Electrochemical measurements and semi-empirical calculations for understanding adsorption of novel cationic Gemini surfactant on carbon steel in H_2SO_4 solution, J. Mol. Struct, 1156 (2018) 473-482.

[65] R.N. Singh, A. Kumar, R.K. Tiwari, P. Rawat, A combined experimental and theoretical (DFT and AIM) studies on synthesis, molecular structure, spectroscopic properties and multiple interactions analysis in a novel Ethyl-4-[2-(thiocarbamoyl) hydrazinylidene]-3, 5-dimethyl-1H-pyrrole-2-carboxylate and its dimer, Spectrochimica Acta Part A: Molecular and Biomolecular Spectroscopy, 112 (2013) 182-190.

[66] H. Jafari, I. Danaee, H. Eskandari, M. RashvandAvei, Combined computational and experimental study on the adsorption and inhibition effects of N2O2 schiff base on the corrosion of API 5L grade B steel in 1 mol/L HCl, Journal of Materials Science & Technology, 30 (2014) 239-252.

[67] M. Messali, H. Lgaz, R. Dassanayake, R. Salghi, S. Jodeh, N. Abidi, O. Hamed, Guar gum as efficient non-toxic inhibitor of carbon steel corrosion in phosphoric acid medium: Electrochemical, surface, DFT and MD simulations studies, Journal of Molecular Structure, 1145 (2017) 43-54.

[68] L.M. Rodríguez-Valdez, W. Villamisar, M. Casales, J.G. Gonzalez-Rodriguez, A. Martínez-Villafañe, L. Martinez, D. Glossman-Mitnik, Computational simulations of the molecular structure and corrosion properties of amidoethyl, aminoethyl and hydroxyethyl imidazolines inhibitors, Corrosion science, 48 (2006) 4053-4064.

[69] K. Babic´-Samardz˘ija, K.F. Khaled, N. Hackerman, Appl. Surf. Sci. 240, 327–340 (2005)

[70] H. Lgaz, O. Benali, R. Salghi, S. Jodeh, M. Larouj, O. Hamed, M. Messali, S. Samhan, M. Zougagh, H. Oudda, Pyridinium derivatives as corrosion inhibitors for mild steel in 1M HCl: electrochemical, surface and quantum chemical studies. Der Pharma Chem. 8 (2016) 172–190. Brought to you by| Google Googlebot-Web Crawler SEO Said et al.: C11H19N2I| 3 phthalazinone derivatives and their antihypertensive activities, Eur. J. Med. Chem, 39 (2004) 1089-1095.

[71] A.Y. Musa, A.A.H. Kadhum, A.B. Mohamad, M.S. Takriff, Experimental and theoretical study on the inhibition performance of triazole compounds for mild steel corrosion, Corrosion Science, 52 (2010) 3331-3340.

[72] X. Li, S. Deng, H. Fu, Blue tetrazolium as a novel corrosion inhibitor for cold rolled steel in hydrochloric acid solution, Corrosion Science, 52 (2010) 2786-2792.

Table 1. Chemical composition *(wt %)* of mild steel DC06EK.

Element	C	Si	Mn	P	Al	Ti	Ni	Fe
wt %	0.0004	0.007	0.190	0.0008	0.069-0.08	0.17	0.0089	Balance

Table 2. Calculated values of corrosion rate (v_{corr}) and inhibition efficiency (%IE) for mild steel corrosion in 1 M HCl in the absence and presence of (DDP) at 30 °C.

Inhibitor	***Conc. (mol/l)***	***v_{corr} (mg/cm^2.h)***	***%IE***
DDP	**Blank**	**0.50**	---
	10^{-5}	0.074	85.20
	5×10^{-5}	0.036	92.80
	10^{-4}	0.030	94.00
	5×10^{-4}	0.017	96.60

Table 3. Calculated values of corrosion rate (v_{corr}) and inhibition efficiency (%IE) for mild steel corrosion in 1 M HCl in the absence and presence of (DDP) at 30, 40, 50, 60 °C.

Concentration Mol/l		***v_{corr} (mg/cm^2.h)***				***Inhibition efficiency (%IE)***			
		30°C	***40 °C***	***50 °C***	***60 °C***	***30°C***	***40 °C***	***50 °C***	***60 °C***
	Blank	**0.5**	**0.70**	**1.50**	**3.50**	---	---	---	---
DDP	10^{-5}	0.074	0.100	0.350	1.010	85.20	85.71	76.66	71.14
	5×10^{-5}	0.036	0.068	0.180	0.653	92.80	90.28	88.00	81.34
	10^{-4}	0.030	0.051	0.120	0.380	94.00	92.71	92.00	89.14
	5×10^{-4}	0.017	0.026	0.081	0.130	96.60	96.30	94.60	96.30

Table 4. Activation parameters of the dissolution of mild steel in 1M HCl in the absence and presence of different concentrations of (DDP).

Inhibitor	***Concentration (mol/l)***	***A***	***R^2***	***E_a (kJ/mol)***
DDP	Blank	1.23×10^{9}	0.9841	54.84
	10^{-5}	6.00×10^{11}	0.9755	75.50
	5×10^{-5}	2.22×10^{12}	0.9883	80.41
	10^{-4}	3.62×10^{10}	0.9854	70.50
	5×10^{-4}	3.75×10^{8}	0.9820	60.21

Table 5. Affect of immersion time on corrosion rate of mild steel in 1 M HCl in the absence and presence of (DDP, 5×10^{-4} M) at T=30 °C.

Immersion time (min)	v_{corr} *(mg/cm^2.h) Blank*	v_{corr} *(mg/cm^2.h) DDP (5×10^{-4} M)*	*Inhibition Efficiency (%IE)*
30	0.56	0.03046	94.56
60	0.5	0.01740	96.52
120	0.38	0.02166	94.30
240	0.37	0.01200	96.76
360	0.40	0.00960	97.60
480	0.42	0.00840	98.00
1440	0.52	0.00980	98.11

Table 6. Thermodynamic parameters of the adsorption of (DDP) on mild steel surface in 1 M HCl 30, 40, 50 and 60 °C.

Inhibitor	*T (°C)*	R^2	*Slope*	K_{ads}	ΔG_{ads} *(kJ/mol)*
DDP	30	0.9999	1.030	4.60×10^5	**-43.00**
	40	0.9999	1.034	3.35×10^5	**-43.55**
	50	0.9999	1.053	3.00×10^5	**-44.65**
	60	0.9990	1.026	1.31×10^5	**-43.74**

Table 7. Potentiodynamic polarization parameters for the corrosion of MS in 1 M HCl without and with different concentrations of (DDP) at 30 °C.

DDP (mol / l)	***E_{corr} (mV vs. SCE)***	***I_{corr} (uA /cm ^{2})***	***B_a (mV/dec)***	***$-B_c$ (mV/dec)***	***%IE***
Blank	-583.3	290	73.1	95.6	…
10^{-5}	-531.0	39.4	71.6	149.5	86.41
5 x 10^{-5}	-524.4	30.0	52.7	121.3	89.65
10^{-4}	-494.0	26.5	68.2	219.3	90.86
5 x 10^{-4}	-468.1	13.1	71.0	137.5	95.50

Table 8. Impedance parameters and inhibition efficiency for the corrosion of mild steel in 1 M HCl with different concentrations of (DDP) at 30 °C.

Conc.	***R_{ct} (Ω. cm^2)***	***n***	***C_{dl} (µF/cm^2)***	***%IE***
Blank	42.11	0.89	755.80	….
10^{-5}	347.60	0.84	81.48	87.88
5 × 10^{-5}	571.70	0.78	69.60	92.63
10^{-4}	776.30	0.86	64.74	94.60
5 × 10^{-4}	893.40	0.85	126.8	95.30

Table 9. Calculated quantum chemical parameters of (DDP) pyrazole derivative.

Inh	***µ (D)***	***E_{tot} (Har)***	***E_{HOMO} (eV)***	***E_{LUMO} (eV)***	***ΔE (eV)***	***V (cm^3/mol)***
DDP	9.72	-1526.83	-5.08	-1.94	3.14	340.57

Table 10. The Fukui indices (DDP) pyrazole estimated using POP=NPA analysis.

Atom k	f_k^+	f_k^-	*Atom k*	f_k^+	f_k^-
C 1	-0.01254	-0.00414	***C 15***	0.00261	-0.00057
C 2	0.00644	-0.00776	***N 16***	0.00977	0.08172
N 3	-0.00491	0.05164	***C 17***	-0.00353	-0.01286
N 4	**0.11707**	0.02524	***C 18***	-0.00296	-0.01239
C 5	0.06665	0.01542	***C 19***	**0.14144**	0.02520
C 6	0.01070	-0.02174	***C 20***	-0.02612	0.02981
S 7	**0.12452**	**0.16483**	***C 21***	0.03801	0.01517
N 8	0.02312	0.02042	***C 22***	0.00970	0.02845
C 9	0.06110	0.03695	***C 23***	0.07868	0.02368
C 10	-0.02739	0.03681	***C 24***	0.00371	0.02494
C 11	-0.00734	-0.00361	***C 25***	0.06416	0.01205
C 12	0.00503	0.02657	***N 26***	0.02993	0.07652
C 13	0.01589	0.00956	***C 27***	-0.00836	-0.01252
C 14	0.00963	0.03630	***C 28***	-0.00839	-0.01262

Table 11. Interaction and binding energy values for (DDP) using DFT//B3LYP/6-31G* calculations

Systems	**Interaction energy (kcal/mol)**	**Binding energy (kcal/mol)**
Fe-DDP/Vacuum	-21.11	21.11
Fe-DDP/HCl solution	-27.01	27.01

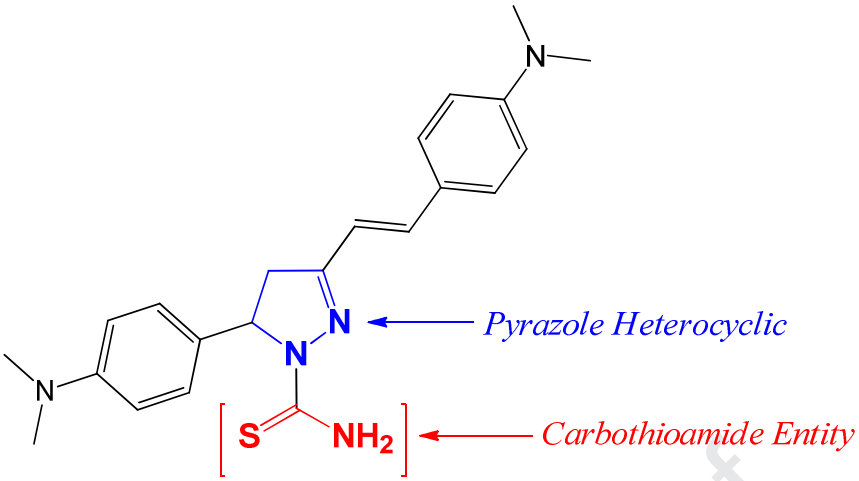

Fig. 1. Molecular structure of (DDP) inhibitor

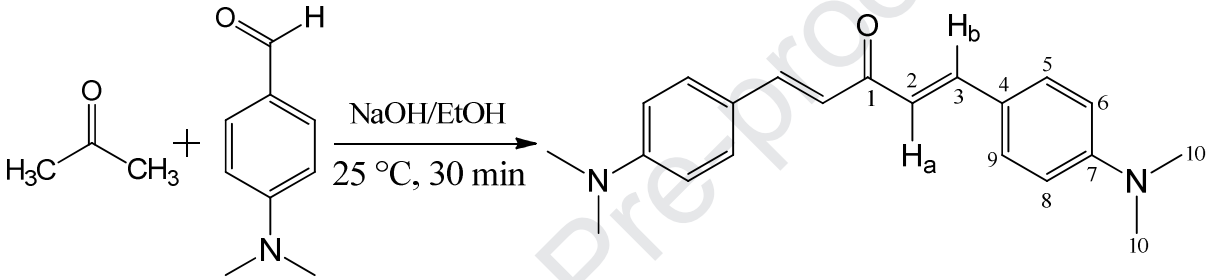

Scheme 1. Synthesis of the intermediate dibenzalacetone (4-DBA)

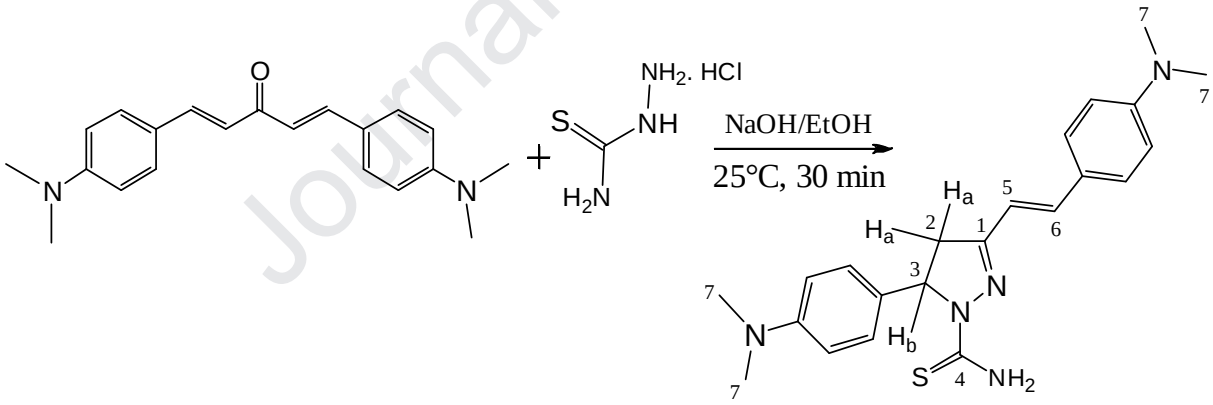

Scheme 2. Synthesis of pyrazole carbothioamide derivative (DDP)

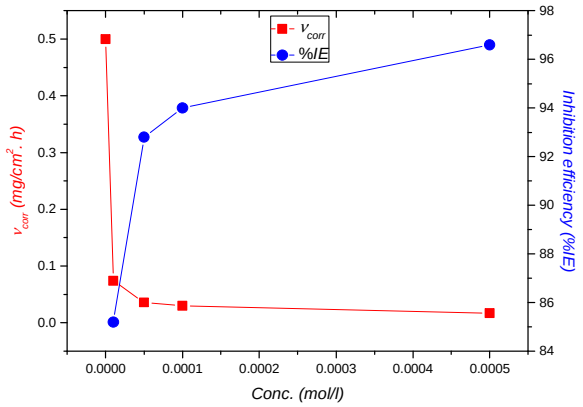

Fig. 2. Relationship of corrosion rate (v_{corr}) and inhibition efficiency (%IE) with concentration of (DDP) in 1 M HCl at 30 °C.

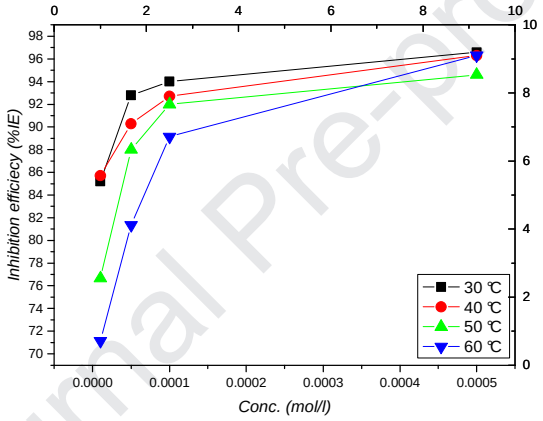

Fig. 3. Relationship between inhibition efficiency (%IE) and concentration of (DDP) in 1 M HCl at different temperatures

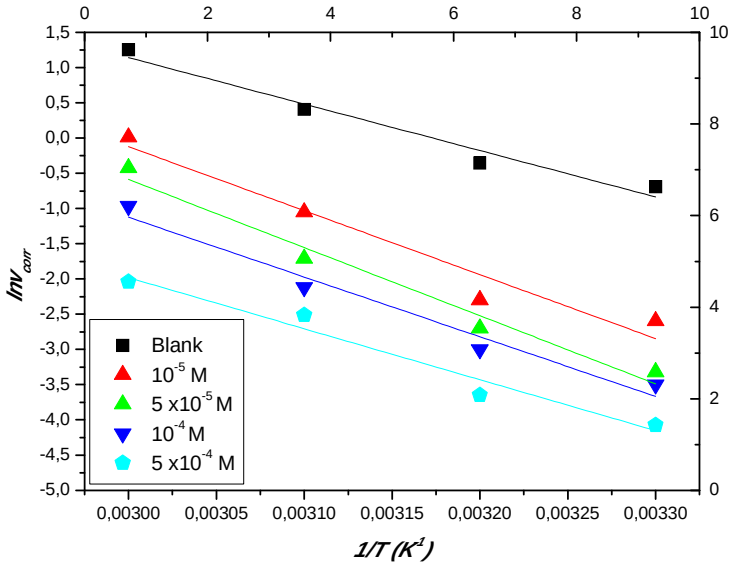

Fig. 4. Arrhenius plot for mild steel corrosion in 1 M HCl in the absence and presence of different concentrations of (DDP).

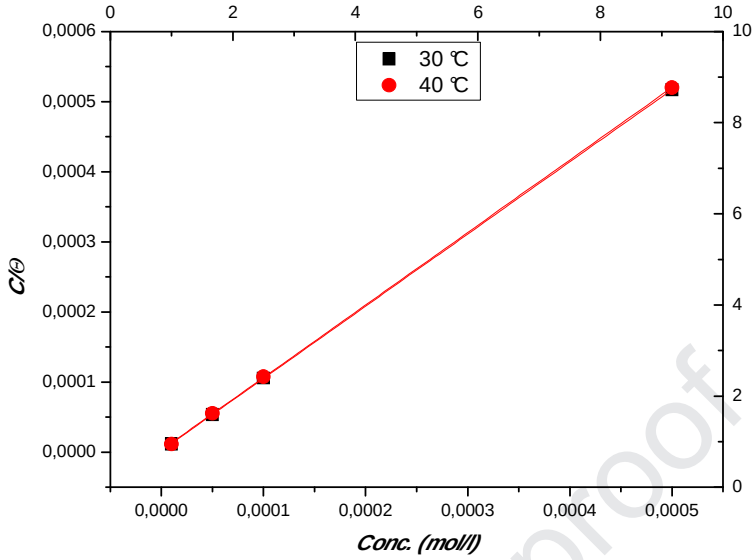

Fig. 5. Langmuir isotherm adsorption modes of (DDP) on the MS surface in 1 M HCl at 30 °C and 40 °C.

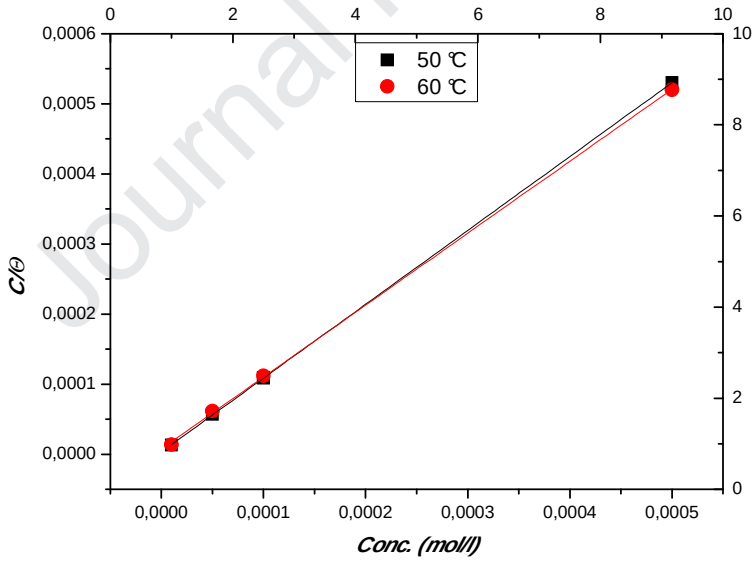

Fig. 6. Langmuir isotherm adsorption modes of (DDP) on the MS surface in 1 M HCl at 50 °C and 60 °C.

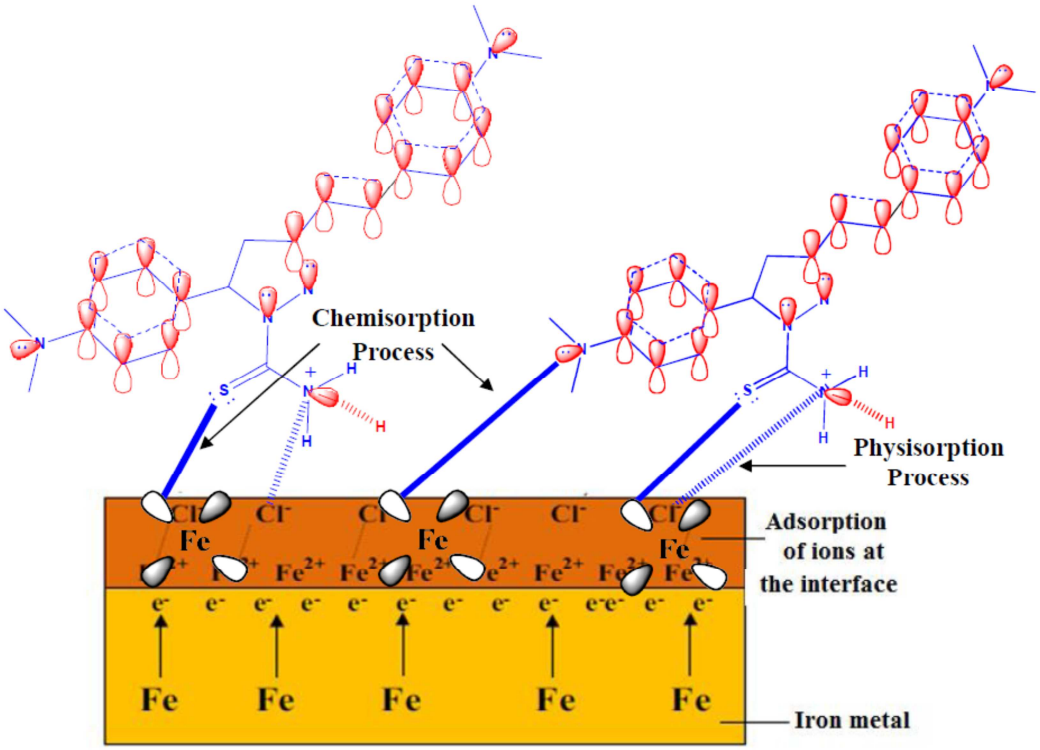

Fig. 7. Mechanism of corrosion inhibition of MS in the presence of (DDP) in 1 M HCl

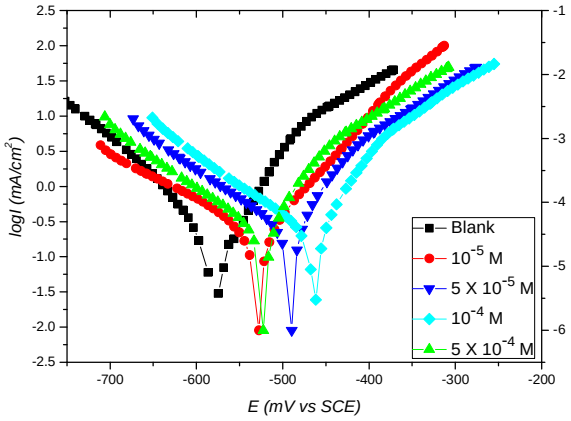

Fig. 8. Polarization curves for MS in 1 M HCl with different concentrations of (DDP) at 30 °C.

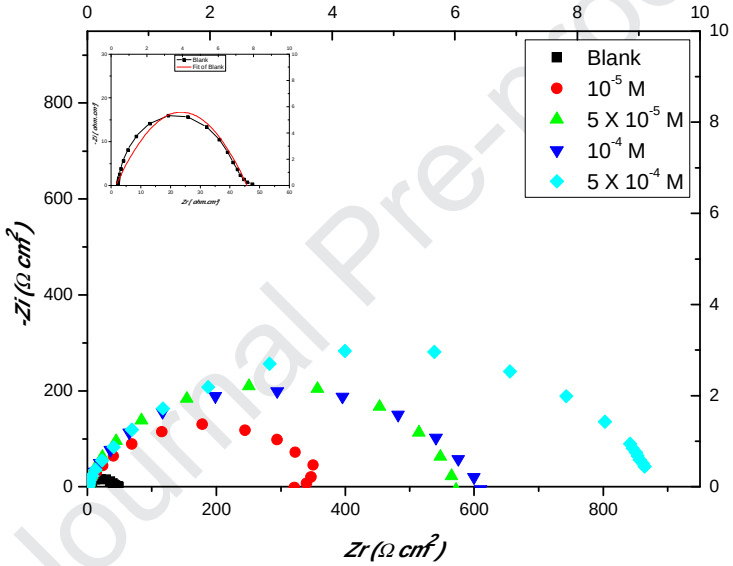

Fig. 9. Nyquist plots for MS in 1 M HCl solution in the absence and in the presence of different concentrations of (DDP) at 30 °C

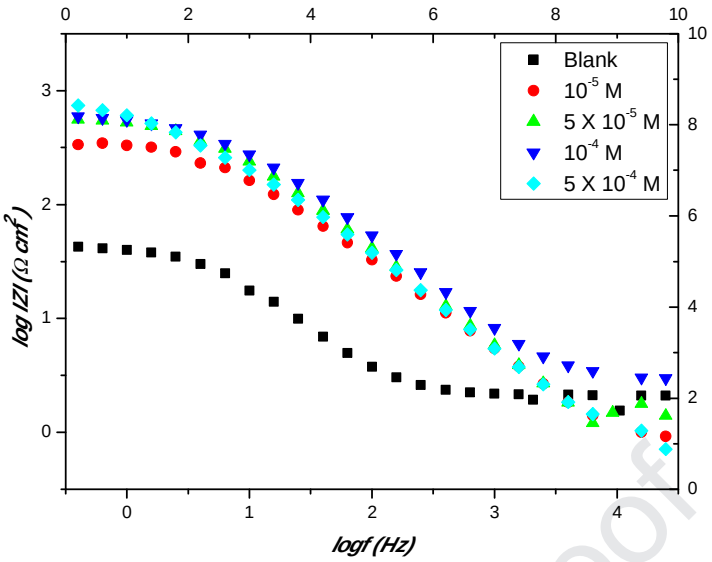

Fig. 10. Bode Modulus plots for MS in 1 M HCl solution in the absence and in the presence of different concentrations of (DDP) at 30 °C

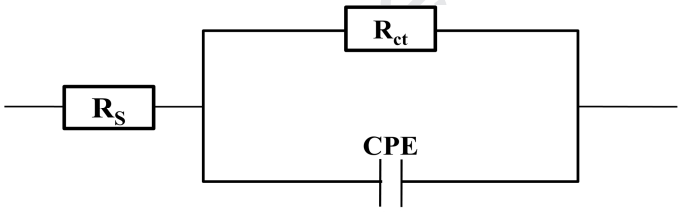

Fig. 11. The equivalent circuit of the impedance spectra obtained for (DDP) pyrazole in 1 M HCl

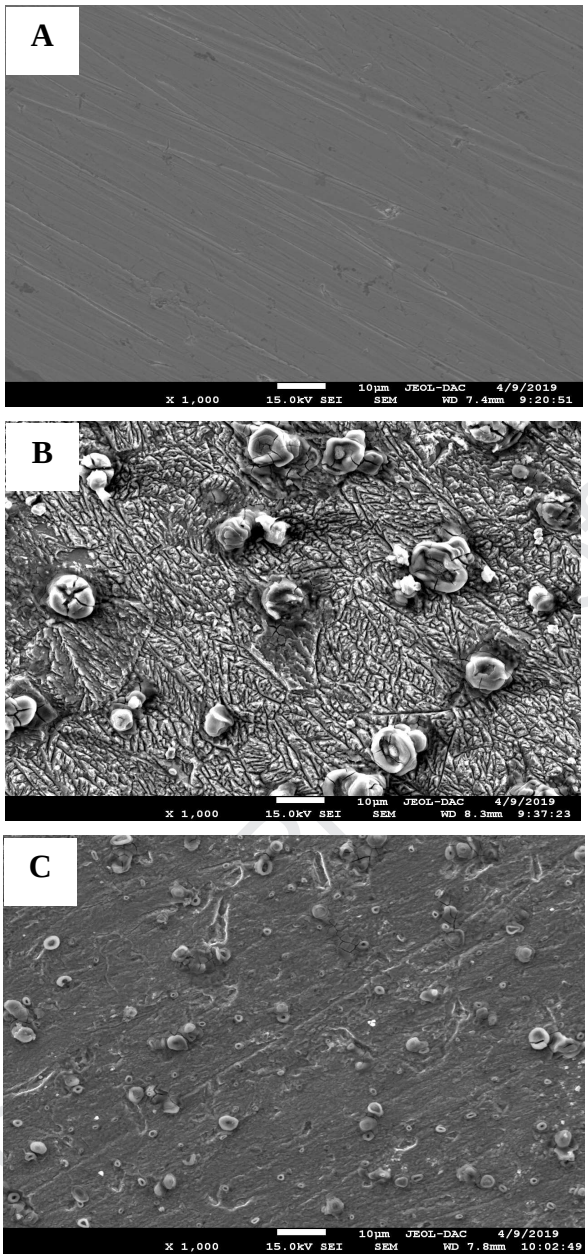

Fig. 12. SEM analysis of MS surface: (A) before immersion; (B) after 24 h of immersion in 1 M HCl at 30 °C; (C) after 24 h of immersion in 1 M HCl + 5×10^{-4} M (DDP) at 30 °C.

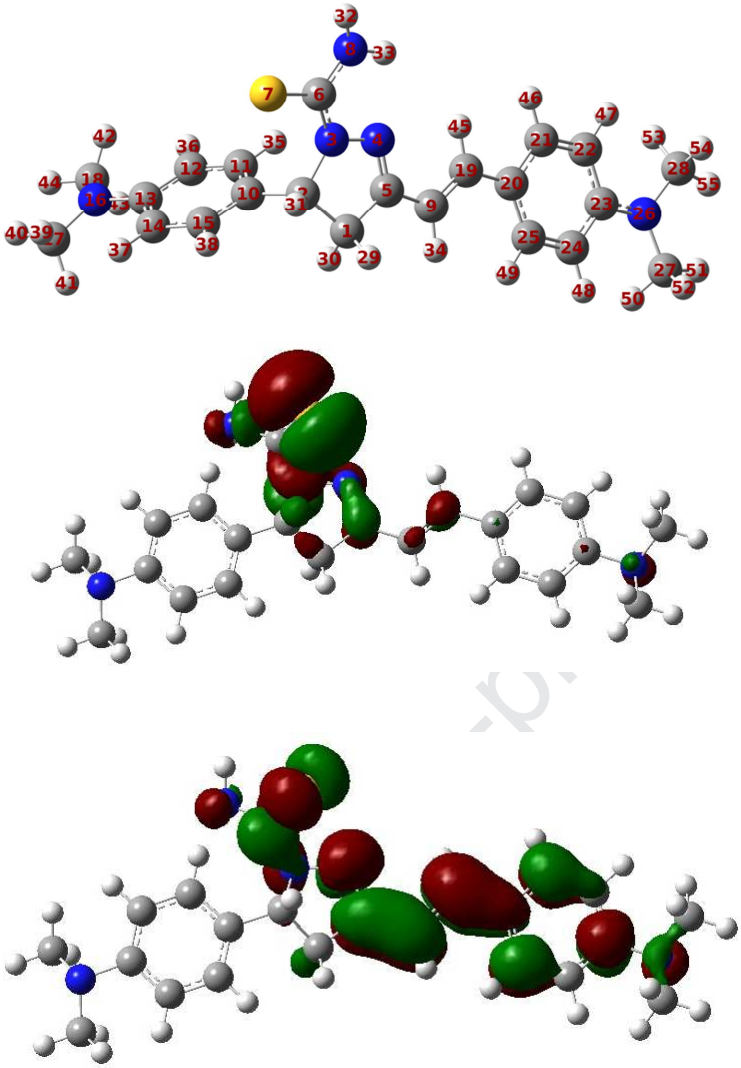

Fig. 13. The optimized structure, HOMO and LUMO electronic distribution of (DDP) pyrazole obtained from B3LYP/6-31G* method

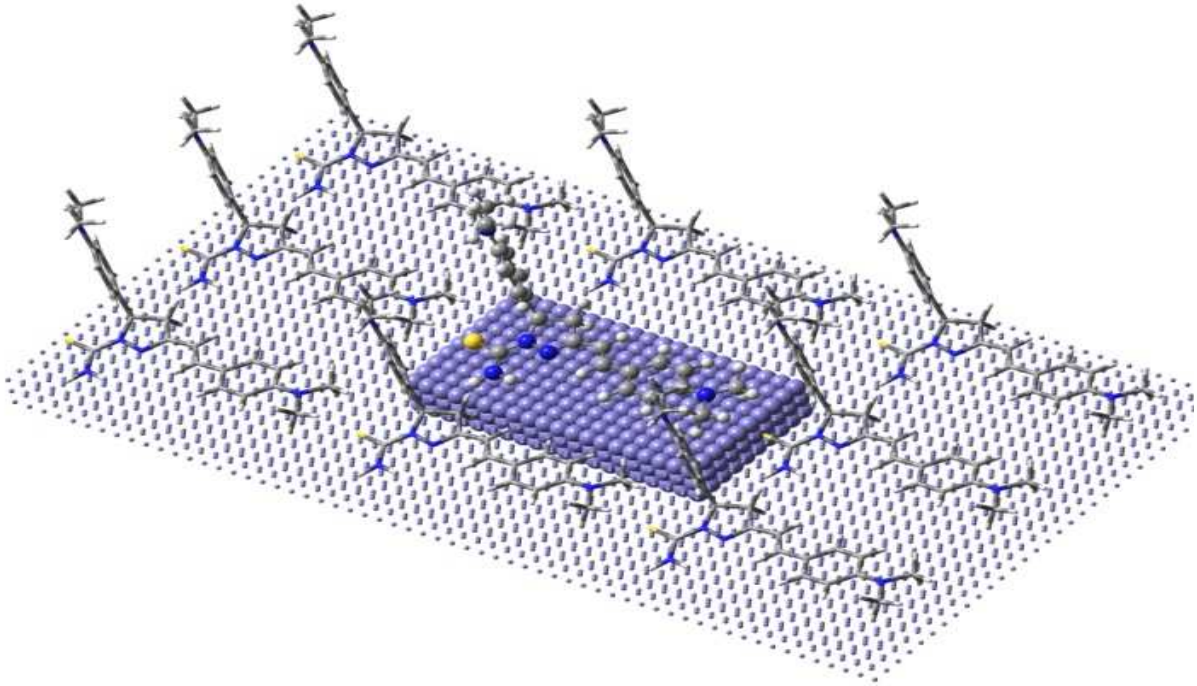

Fig. 14. The most stable configuration for adsorption of (DDP) pyrazole on the steel surface

- A new pyrazole (DDP) was synthesized and studied as corrosion inhibitor.
- Adsorption of DDP inhibitor follows a Langmuir isotherm.
- The formed organic film was examined by SEM analysis
- DFT calculations are in good agreement with experimental results